

Table 2 Top 20 upregulated genes in F3 cells following stable expression of neurogenin 1

No.	Gene symbol	Fold change	Entrez gene ID	Gene name	Putative function
1	LGR5	166.623	8549	Leucine-rich repeat-containing G protein-coupled receptor 5	An orphan G protein-coupled receptor of the glycoprotein hormone receptor subfamily
2	GAS2	32.861	2620	Growth arrest-specific 2	A caspase-3 substrate that plays a role in regulating cell shape changes during apoptosis
3	FABP3	32.739	2170	Fatty acid-binding protein 3, muscle and heart (mammary-derived growth inhibitor)	A protein involved in intracellular metabolism of long-chain fatty acids and modulation of cell growth and proliferation
4	TMEFF2	28.233	23671	Transmembrane protein with EGF-like and two follistatin-like domains 2	A secreted protein with a EGF-like domain that promotes survival of hippocampal and mesencephalic neurons
5	LRRN3	24.284	54674	Leucine-rich repeat neuronal 3	An integral membrane protein of unknown function
6	SCG2	13.841	7857	Secretogranin II (chromogranin C)	A secretory protein involved in regulation of neurogenesis and angiogenesis
7	MFAP4	13.429	4239	Microfibrillar-associated protein 4	An extracellular matrix protein binding to both collagen and carbohydrate involved in cell adhesion
8	HIST1H4F	11.875	8361	H4 histone, family 2	A member of the histone H4 family that constitutes the nucleosome structure
9	TACR1	11.35	6869	Tachykinin receptor 1	A neurokinin receptor selective for substance P
10	COL3A1	10.828	1281	Collagen, type III, alpha 1	The pro-alpha 1 chains of type III collagen that constitutes a major component of the extracellular matrix
11	SDPR	9.975	8436	Serum deprivation response (phosphatidylserine-binding protein)	A calcium-independent phospholipid-binding protein that serves as a substrate of protein kinase C
12	TMTC2	9.744	160335	Transmembrane and tetratricopeptide repeat containing 2	An integral membrane protein of unknown function
13	FGF9	9.38	2254	Fibroblast growth factor 9 (glia-activating factor)	A member of the FGF family whose expression is dependent on Sonic hedgehog signaling
14	ASS1	8.813	445	Argininosuccinate synthetase 1	The enzyme that catalyzes the penultimate step of the arginine biosynthetic pathway
15	S100A4	8.555	6275	S100 calcium binding protein A4	A member of the S100 family of proteins involved in motility, invasion, and tubulin polymerization
16	LIX1	7.99	167410	Lix1 homolog (chicken)	A protein involved in RNA metabolism that has an essential function for motor neuron survival
17	FAM65B	7.974	9750	Family with sequence similarity 65, member B	a protein involved in myogenic cell differentiation
18	NOG	7.65	9241	Noggin	A secreted protein that plays a principal role in creating morphogenic gradients by antagonizing bone morphogenetic proteins
19	C1orf115	7.571	79762	Chromosome 1 open reading frame 115	An integral membrane protein of unknown function
20	CYSLTR2	7.23	57105	Cysteinyl leukotriene receptor 2	A G protein-coupled receptor for cysteinyl leukotrienes

Genome-wide gene expression profiling of F3-WT and F3-Ngn1 was performed by using two sets of Human Gene 1.0 ST Array for each, followed by two comparisons composed of WT array-1 (F3-WT-1) versus Ngn1 array-1 (F3-Ngn1-1) and WT array-2 (F3-WT-2) versus Ngn1 array-2 (F3-Ngn1-2). Top 20 upregulated genes in F3-Ngn1 cells are shown with fold change derived from the comparison between F3-WT-2 and F3-Ngn1-2

genes directly linked to the 537 genes. Subsequently, we performed the “N-points to N-points” search by starting from Ngn1 and ending with the set of 787 genes via the shortest route connecting starting and ending points. It generated a highly complex molecular network composed of 1,816 fundamental nodes and 7,238 molecular relations (Fig. 6). When the network was referred to the canonical pathways of the KeyMolnet library, the generated network

has the most significant relationship with transcriptional regulation by nuclear factor kappa-B (NF- κ B) with the score of 59.9 and score (p) = 9.467E-019. This was followed by transcriptional regulation by cyclic AMP-response element-binding protein (CREB) in the second rank with the score of 52.3 and score (p) = 1.771E-016, transcriptional regulation by vitamin D receptor (VDR) in the third rank with the score of 45.8 and score (p) = 1.582E-014, transcriptional

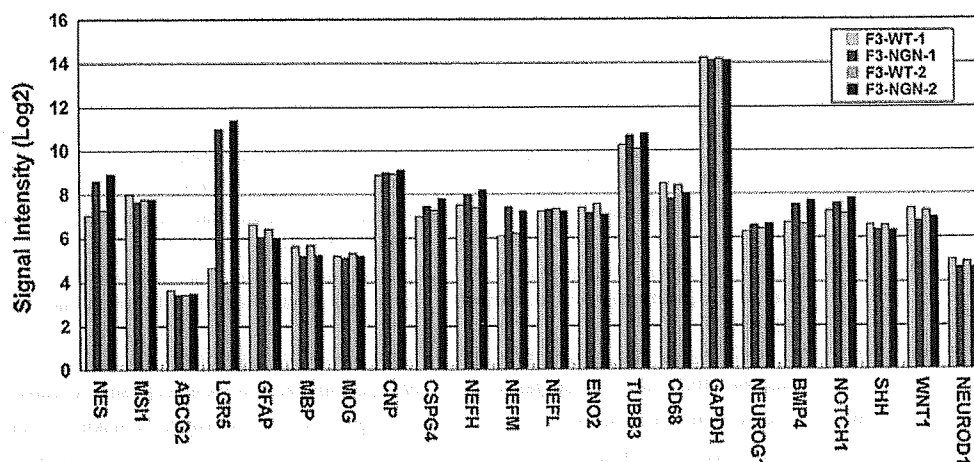


Fig. 3 Gene expression profiles of NSC, neuronal and glial markers. Genome-wide gene expression profiling of F3-WT and F3-Ngn1 was performed by using two sets of Human Gene 1.0 ST Array for each, followed by two comparisons composed of WT array-1 (F3-WT-1; the first column) versus Ngn1 array-1 (F3-Ngn1-1; the second column) and WT array-2 (F3-WT-2; the third column) versus Ngn1 array-2 (F3-Ngn1-2; the fourth column). Signal intensities of NSC, neuronal and glial marker genes are expressed as log 2 after normalization. *NES* nestin, *MSH* musashi homolog 1, *ABCG2* ATP-binding cassette, subfamily G member 2, *LGR5* leucine-rich repeat-containing G protein-coupled receptor 5, *GFAP* glial fibrillary acidic

protein, *MBP* myelin basic protein, *MOG* myelin oligodendrocyte glycoprotein, *CNP*, 2'3'-cyclic nucleotide 3' phosphodiesterase, *CSPG4* chondroitin sulfate proteoglycan 4 (NG2), *NEFH* neurofilament heavy polypeptide, *NEFM* neurofilament medium polypeptide, *NEFL* neurofilament light polypeptide, *ENO2* enolase 2 (NSE), *TUBB3* tubulin beta 3, *GAPDH* glyceraldehyde-3-phosphate dehydrogenase (G3PDH), *NEUROG1* neurogenin 1, *BMP4* bone morphogenic protein 4, *NOTCH1* notch homolog 1, *SHH* sonic hedgehog homolog, *WNT1* wingless-type MMTV integration site family member 1, and *NEUROD1* neurogenic differentiation 1. A robust upregulation of *LGR5* is evident in both F3-Ngn1-1 and F3-Ngn1-2

regulation by hypoxia-inducible factor (HIF) in the fourth rank with the score of 35.7 and score (p) = $1.781E-011$, transcriptional regulation by glucocorticoid receptor (GR) in the fifth rank with the score of 31.0 and score (p) = $4.779E-010$, and the complement activation pathway in the sixth rank with the score of 20.5 and score (p) = $6.589E-007$. Thus, the molecular network of the genes differentially expressed between F3-WT and F3-Ngn1 involves the complex interaction of networks regulated by multiple transcription factors.

Gene Annotation Analysis Suggested Multifunctional Changes in F3-Ngn1 Cells

We studied functional annotation terms overrepresented in 588 DEG by using the web-accessible program named DAVID. By importing the list of Entrez Gene ID, DAVID identified top 20 enriched gene ontology (GO) terms in the list of 250 upregulated genes, most of which are related to development and morphogenesis (Table 4). In contrast, top 20 enriched GO terms in the list of 338 downregulated genes were chiefly composed of the molecules closely associated with extracellular matrix and adhesion (Table 4). Thus, gene annotation analysis suggested that stable expression of a single gene *Ngn1* in F3 cells induces multifunctional changes that potentially affect the differentiation of human NSC.

Discussion

Recently, we established an immortalized human NSC clone named HB1.F3, which could serve as an unlimited source for cell replacement therapy of various neurological diseases (Kim 2004; Kim and de Vellis 2009). *Ngn1* is a proneural bHLH transcription factor that promotes neuronal differentiation but inhibits glial differentiation of rodent NSC and NPC (Morrison 2001; Sun et al. 2001). In the present study, to investigate a role of *Ngn1* in human NSC differentiation, we established a clone derived from F3 stably overexpressing *Ngn1*. Genome-wide gene expression profiling identified 250 upregulated genes and 338 downregulated genes in F3-Ngn1 versus F3-WT cells. Notably, the expression of *LGR5*, a recently identified marker for intestine and hair follicle stem cells (Barker et al. 2007; Jaks et al. 2008; Sato et al. 2009), was greatly elevated in F3-Ngn1 cells at both mRNA and protein levels. However, transient overexpression of *Ngn1* did not induce upregulation of *LGR5* in F3-WT cells, suggesting that *LGR5* is not a direct transcriptional target of *Ngn1*. KeyMolnet, a bioinformatics tool for analyzing molecular relations on a comprehensive knowledgebase, indicated that the molecular network of differentially expressed genes involves the complex interaction of networks regulated by multiple transcription factors, such as $\text{NF-}\kappa\text{B}$, CREB, VDR, HIF, and GR. Gene annotation analysis

Table 3 Top 20 downregulated genes in F3 cells following stable expression of neurogenin 1

No.	Gene symbol	Fold change	Entrez gene ID	Gene name	Putative function
1	HAS2	0.024	3037	Hyaluronan synthase 2	The enzyme involved in synthesis and transport of hyaluronic acid
2	MMP9	0.044	4318	Matrix metalloproteinase 9 (gelatinase B, 92 kDa gelatinase, 92 kDa type IV collagenase)	The enzyme that degrades type IV and V collagens involved in embryonic development and tissue remodeling
3	C3	0.05	718	Complement component 3	A protein that plays a central role in the activation of complement system
4	LCP1	0.05	3936	Lymphocyte cytosolic protein 1 (L-plastin)	An actin-binding protein that plays a role in cell adhesion-dependent signaling
5	PAPPA	0.068	5069	Pregnancy-associated plasma protein A, pappalysin 1	A secreted metalloproteinase which cleaves insulin-like growth factor binding proteins
6	DSP	0.072	1832	Desmoplakin	A component of functional desmosomes that anchors intermediate filaments to desmosomal plaques
7	SPOCK1	0.075	6695	Sparc/osteonectin, cwcv and kazal-like domains proteoglycan (testican) 1	A chondroitin sulfate/heparan sulfate proteoglycan expressed in the postsynaptic region of hippocampal pyramidal neurons
8	TRIM22	0.076	10346	Tripartite motif-containing 22	A member of the tripartite motif family induced by interferon and mediates interferon's antiviral effects
9	CCND2	0.087	894	Cyclin D2	A protein that forms a complex with CDK kinases involved in cell cycle G1/S transition
10	IL6	0.088	3569	Interleukin 6 (interferon, beta 2)	An immunoregulatory cytokine that functions in inflammation and the maturation of B cells
11	CD82	0.092	3732	CD82 molecule	A membrane glycoprotein activated by p53 involved in suppression of metastasis
12	SLC43A3	0.093	29015	Solute carrier family 43, member 3	An integral membrane protein of the SLC43A transporter family
13	GREM1	0.093	26585	Gremlin 1, cysteine knot superfamily, homolog (<i>Xenopus laevis</i>)	A member of bone morphogenic protein antagonist family expressed in the neural crest
14	INHBA	0.095	3624	Inhibin, beta A	A growth/differentiation factor for various cell types by acting as a homodimer (activin A) or a heterodimer (activin A-B)
15	ITGB3	0.095	3690	Integrin, beta 3 (platelet glycoprotein IIIa, antigen CD61)	A subunit of integrins involved in cell adhesion and cell-surface-mediated signaling
16	FAP	0.097	2191	Fibroblast activation protein, alpha	A homodimeric integral membrane gelatinase involved in epithelial-mesenchymal interactions during development
17	C1S	0.101	716	Complement component 1, s subcomponent	A major constituent of the human complement subcomponent C1 that associates with C1r and C1q to yield the first component of the serum complement system
18	PXDN	0.103	7837	Peroxidasin homolog (Drosophila)	An extracellular matrix-associated peroxidase involved in extracellular matrix consolidation
19	C4orf18	0.103	51313	Chromosome 4 open reading frame 18	A Golgi apparatus membrane of unknown function
20	CFH	0.104	3075	Complement factor H	Q serum glycoprotein that regulates the function of the alternative complement pathway

Genome-wide gene expression profiling of F3-WT and F3-Ngn1 was performed by using two sets of Human Gene 1.0 ST Array for each, followed by two comparisons composed of WT array-1 (F3-WT-1) versus Ngn1 array-1 (F3-Ngn1-1) and WT array-2 (F3-WT-2) versus Ngn1 array-2 (F3-Ngn1-2). Top 20 downregulated genes in F3-Ngn1 cells are shown with fold change derived from the comparison between F3-WT-2 and F3-Ngn1-2

suggested that GO terms of development and morphogenesis are enriched in upregulated genes, while those of extracellular matrix and adhesion are enriched in downregulated genes. These results suggest that stable expression of a single gene Ngn1 in F3 cells induces not simply

neurogenic but multifunctional changes that potentially affect the differentiation of human NSC via a reorganization of complex gene regulatory networks.

LGR5, an orphan G protein-coupled receptor alternatively named GRP49 with structural similarity to the

Fig. 4 Real-time RT-PCR and Western blot analysis. cDNA prepared from F3-WT and F3-Ngn1 cells was processed for real-time RT-PCR using primer sets listed in Table 1. Total protein extract was processed for western blot with anti-LGR5 antibody. The panels (a–e) represent real-time RT-PCR of **a** LGR5, **b** GAS2, **c** HAS2, and **d** MMP9, and western blot of (**e**, upper panel) LGR5 and (**e**, lower panel) Hsp60, an internal control for protein loading

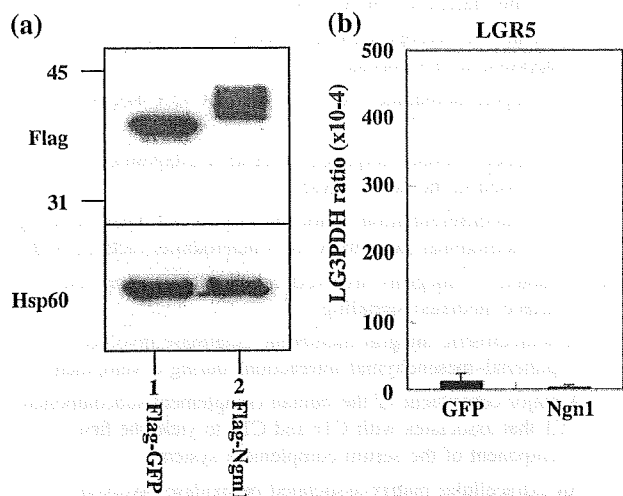
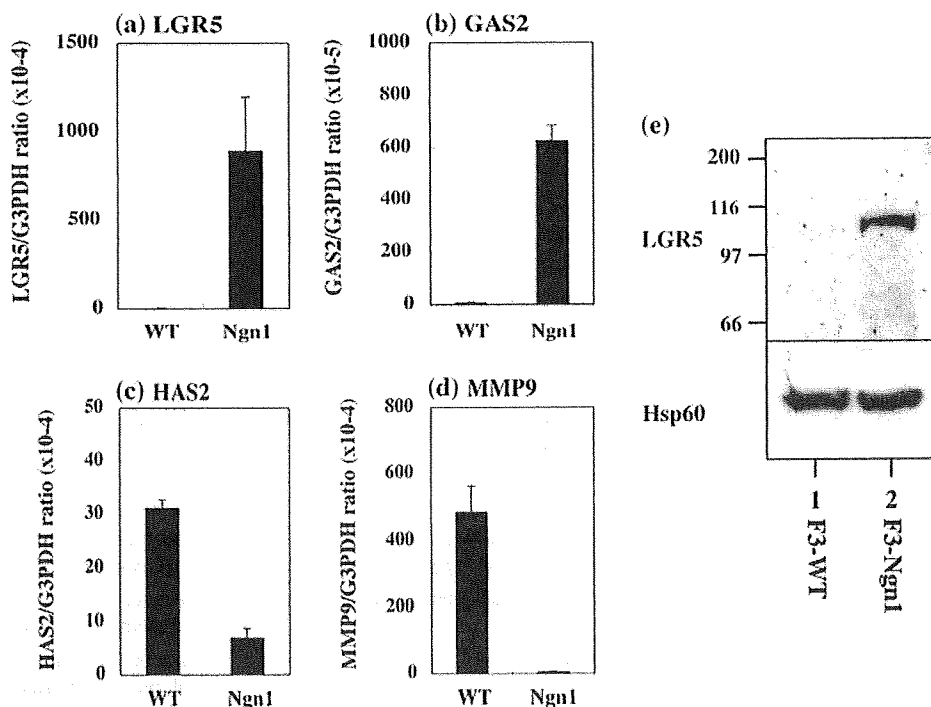


Fig. 5 Transient overexpression of Ngn1 did not induce upregulation of LGR5 in F3-WT cells. Expression vectors of Flag-tagged Ngn1 or GFP were transfected in F3-WT cells. At 48 h after transfection, the cells were processed for Western blot analysis of Flag and real-time RT-PCR analysis of LGR5. **a** Western blot analysis. The lanes (1, 2) represent 1 Flag-tagged GFP and 2 Flag-tagged Ngn1. The upper panel indicates Flag-tagged proteins, while the lower panel indicates Hsp60, an internal control for protein loading. **b** Real-time RT-PCR analysis. The left bar represents F3-WT cells with transient overexpression of Flag-tagged GFP, while the right bar represents those with transient overexpression of Flag-tagged Ngn1

glycoprotein hormone receptor family, is recently identified as a marker of adult intestinal stem cells and hair follicle stem cells by lineage-tracing studies (Barker et al. 2007; Jaks et al. 2008; Sato et al. 2009). LGR5 expression

is also identified in the adult human spinal cord and brain at least at mRNA levels (Hsu et al. 1998). At present, the precise physiological function of LGR5 and downstream signaling pathways remain unknown owing to the lack of an identified natural ligand. LGR gene knockout mice showed neonatal lethality due to a breast-feeding defect caused by ankyloglossia, suggesting an involvement of LGR5 in craniofacial development (Morita et al. 2004). A more recent study showed that LGR5 deficiency induces premature differentiation of Paneth cells in the small intestine, accompanied by overactivation of the Wnt pathway, indicating that LGR5 acts as a negative regulator of Wnt (Garcia et al. 2009). A different study revealed that LGR5 is a marker for the sublineage of intestinal stem cells that are responsive to Wnt signals derived from stem cell niche (Ootani et al. 2009). In the populations of intestinal stem cells, LGR5 labels cycling cells, while doublecortin-like kinase-1 (DCLK1) marks quiescent cells (May et al. 2009). Interestingly, the expression of DCLK2, a putative paralog of DCLK1, is elevated with a 3.38-fold increase in F3-Ngn1 cells (Supplementary Table 1).

The interaction between Wnt proteins and Frizzled receptors on the cell surface transduces the signals to β -catenin by inactivating glycogen synthase kinase 3 β (GSK3 β), and stabilized β -catenin is translocated into the nucleus and forms a complex with T-cell factor (TCF) transcription factors to activate transcription of Wnt target genes. Importantly, LGR5 is identified as one of Wnt target genes (Yamamoto et al. 2003), suggesting a key role of LGR5 in establishment of a negative feedback loop in the

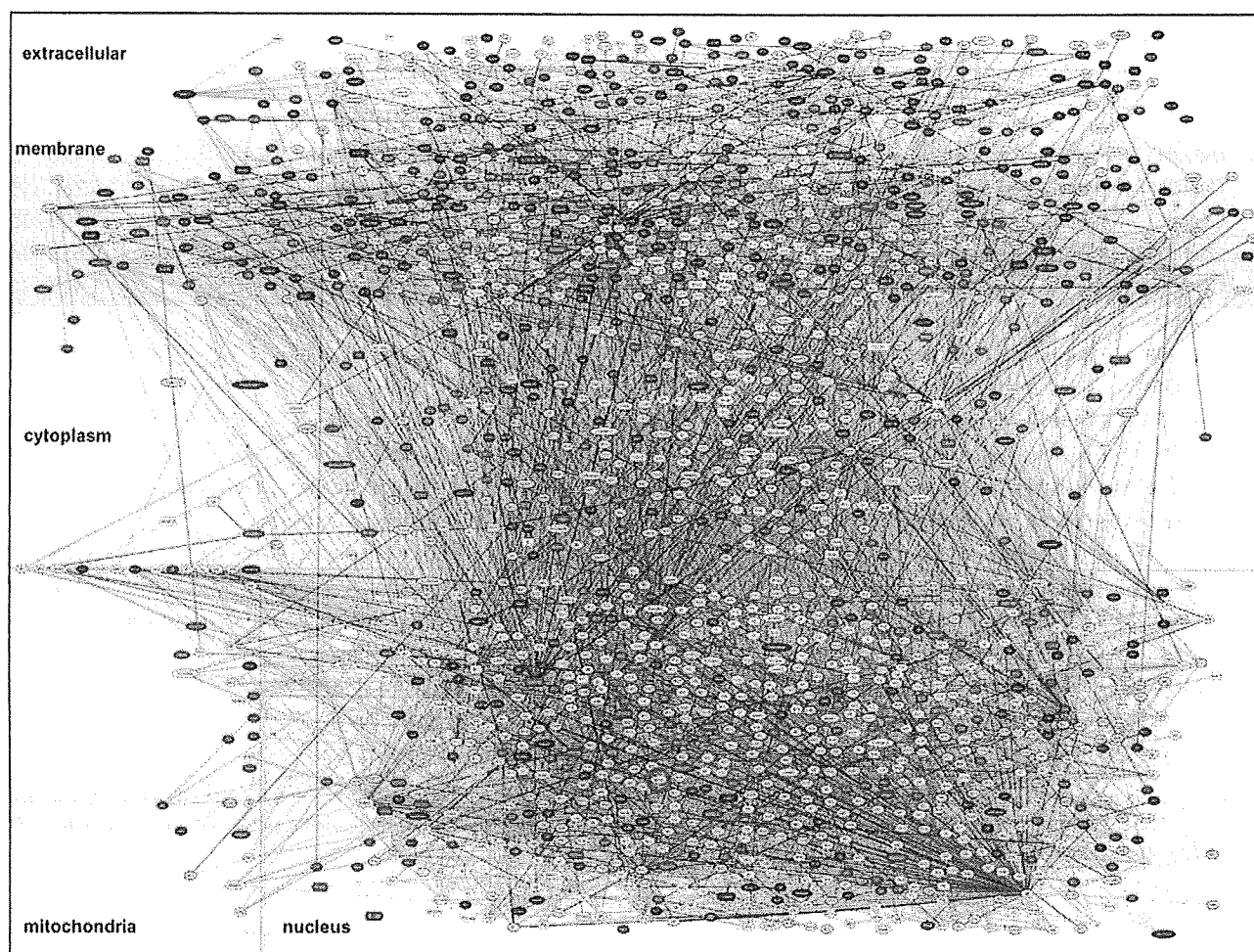


Fig. 6 Molecular network analysis of the genes regulated by stable expression of Ngn1 in F3 cells. The Entrez Gene ID and expression levels of 588 differentially expressed genes (DEG) between F3-WT and F3-Ngn1 cells were imported into KeyMolnet. It extracted 787 genes directly linked to the DEG. The “N-points to N-points” search was performed by starting from Ngn1 and ending with the set of 787 genes via the shortest route connecting starting and ending points. It generated a complex molecular network composed of 1,816 fundamental nodes and 7,238 molecular relations, arranged according to the

subcellular location. *Red nodes* indicate upregulated genes, while *blue nodes* represent downregulated genes. *White nodes* exhibit additional molecules extracted automatically from KeyMolnet contents to establish molecular connections. The connections of *thick lines* represent the core contents, while *thin lines* indicate the secondary contents of KeyMolnet. The molecular relation is indicated by *dash line with arrow* (transcriptional activation), *solid line with arrow* (direct activation), or *solid line without arrow* (direct interaction or complex formation). Ngn1 is highlighted by a *purple circle*

Wnt pathway. In the present study, several Wnt target genes, such as FGF9 (Hendrix et al. 2006) and Dick homolog 1 (DKK1) (Niida et al. 2004), are coordinately upregulated, whereas MMP9 (Wu et al. 2007) is markedly downregulated in F3-Ngn1 (Tables 2 and 3; Supplementary Tables 1 and 2). FGF9 inhibits astrocyte differentiation of adult mouse NPC (Lum et al. 2009). One of us (SUK) recently found that DKK1 is a negative regulator of Wnt signaling in HB1.F3 cells (Ahn et al. 2008). MMP9 plays a central role in migration of adult NSC and NPC (Barkho et al. 2008). Interestingly, Ngn1 is also identified as a target of Wnt signaling, and it inhibits the self-renewal capacity of mouse cortical neural precursor cells

(Hirabayashi et al. 2004). The expression of LGR5 is also controlled by the sonic hedgehog (SHH) signaling pathway (Tanese et al. 2008). SHH promotes Ngn1 expression in trigeminal neural crest cells (Ota and Ito 2003). Importantly, both Wnt and SHH signaling pathways play a central role in NSC development and differentiation (Prakash and Wurst 2007). Therefore, F3-Ngn1 cells might serve as a valuable tool for screening natural ligands of LGR5 that potentially affect the human NSC differentiation via Wnt and SHH signaling pathways, although it remains to be investigated whether a specialized subset of LGR5⁺ NSC exists in vivo in the adult human central nervous system (CNS).

Table 4 Functional annotation terms of upregulated and downregulated genes in F3-Ngn1 cells

No.	Top 20 enriched GO terms in upregulated genes	<i>P</i> value	Top 20 enriched GO terms in downregulated genes	<i>P</i> value
1	GO:0048513~organ development	4.71E-08	GO:0044421~extracellular region part	1.66E-24
2	GO:0048731~system development	5.15E-08	GO:0005576~extracellular region	4.49E-22
3	GO:0048856~anatomical structure development	1.32E-07	GO:0005578~proteinaceous extracellular matrix	5.78E-15
4	GO:0007275~multicellular organismal development	1.02E-06	GO:0031012~extracellular matrix	9.50E-15
5	GO:0032502~developmental process	1.73E-06	GO:0009605~response to external stimulus	9.65E-14
6	GO:0009887~organ morphogenesis	1.96E-06	GO:0005615~extracellular space	1.42E-12
7	GO:0001501~skeletal development	4.29E-05	GO:0009611~response to wounding	2.42E-12
8	GO:0009653~anatomical structure morphogenesis	5.80E-05	GO:0022610~biological adhesion	3.08E-12
9	GO:0050793~regulation of developmental process	1.46E-04	GO:0007155~cell adhesion	3.08E-12
10	GO:0051216~cartilage development	1.78E-04	GO:0048731~system development	7.30E-10
11	GO:0007399~nervous system development	1.97E-04	GO:0006954~inflammatory response	1.24E-09
12	GO:0048754~branching morphogenesis of a tube	2.23E-04	GO:0048856~anatomical structure development	1.38E-09
13	GO:0001657~ureteric bud development	2.37E-04	GO:0032502~developmental process	1.87E-09
14	GO:0032501~multicellular organismal process	2.47E-04	GO:0044420~extracellular matrix part	2.45E-09
15	GO:0048598~embryonic morphogenesis	2.48E-04	GO:0005581~collagen	3.15E-09
16	GO:0030154~cell differentiation	3.15E-04	GO:0007275~multicellular organismal development	1.32E-08
17	GO:0048869~cellular developmental process	3.15E-04	GO:0048513~organ development	2.45E-08
18	GO:0000786~nucleosome	3.33E-04	GO:0005509~calcium ion binding	4.38E-08
19	GO:0043583~ear development	3.42E-04	GO:0005125~cytokine activity	6.33E-08
20	GO:0001763~morphogenesis of a branching structure	3.42E-04	GO:0006950~response to stress	1.21E-07

Functional annotation terms overrepresented in the list of 588 genes differentially expressed between F3-WT and F3-Ngn1 cells were searched on the web-accessible program named DAVID. Top 20 enriched gene ontology (GO) terms in 250 upregulated genes and top 20 enriched GO terms in 338 downregulated genes are shown with GO ID and *P* value

Acknowledgments This work was supported by a research grant to J-IS from the High-Tech Research Center Project, the Ministry of Education, Culture, Sports, Science and Technology (MEXT), Japan (S0801043), and from Research on Intractable Diseases, the Ministry of Health, Labour and Welfare of Japan. The microarray data are available from Gene Expression Omnibus (GEO) under the accession number GSE18296.

References

- Ahn SM, Byun K, Kim D, Lee K, Yoo JS, Kim SU, Jho EH, Simpson RJ, Lee B (2008) Olig2-induced neural stem cell differentiation involves downregulation of Wnt signaling and induction of Dickkopf-1 expression. *PLoS One* 3:e3917
- Barker N, van Es JH, Kuipers J, Kujala P, van den Born M, Cozijnsen M, Haegerbarth A, Korving J, Begthel H, Peters PJ, Clevers H (2007) Identification of stem cells in small intestine and colon by marker gene *Lgr5*. *Nature* 449:1003–1007
- Barkho BZ, Munoz AE, Li X, Li L, Cunningham LA, Zhao X (2008) Endogenous matrix metalloproteinase (MMP)-3 and MMP-9 promote the differentiation and migration of adult neural progenitor cells in response to chemokines. *Stem Cells* 26:3139–3149
- Garcia MI, Ghiani M, Lefort A, Libert F, Strollo S, Vassart G (2009) LGR5 deficiency deregulates Wnt signaling and leads to precocious Paneth cell differentiation in the fetal intestine. *Dev Biol* 331:58–67
- Hendrix ND, Wu R, Kuick R, Schwartz DR, Fearon ER, Cho KR (2006) Fibroblast growth factor 9 has oncogenic activity and is a downstream target of Wnt signaling in ovarian endometrioid adenocarcinomas. *Cancer Res* 66:1354–1362
- Hirabayashi Y, Itoh Y, Tabata H, Nakajima K, Akiyama T, Masuyama N, Gotoh Y (2004) The Wnt/ β -catenin pathway directs neuronal differentiation of cortical neural precursor cells. *Development* 131:2791–2801
- Hsu SY, Liang SG, Hsueh AJ (1998) Characterization of two LGR genes homologous to gonadotropin and thyrotropin receptors with extracellular leucine-rich repeats and a G protein-coupled, seven-transmembrane region. *Mol Endocrinol* 12:1830–1845
- Huang da W, Sherman BT, Lempicki RA (2009) Systematic and integrative analysis of large gene lists using DAVID bioinformatics resources. *Nat Protoc* 4:44–57
- Jaks V, Barker N, Kasper M, van Es JH, Snippert HJ, Clevers H, Toftgård R (2008) *Lgr5* marks cycling, yet long-lived, hair follicle stem cells. *Nat Genet* 40:1291–1299
- Kim SU (2004) Human neural stem cells genetically modified for brain repair in neurological disorders. *Neuropathology* 24:159–174
- Kim SU, de Vellis J (2009) Stem cell-based cell therapy in neurological diseases: a review. *J Neurosci Res* 87:2183–2200
- Kim S, Ghil SH, Kim SS, Myeong HH, Lee YD, Suh-Kim H (2002) Overexpression of neurogenin1 induces neurite outgrowth in F11 neuroblastoma cells. *Exp Mol Med* 34:469–475
- Kim S, Yoon YS, Kim JW, Jung M, Kim SU, Lee YD, Suh-Kim H (2004) Neurogenin1 is sufficient to induce neuronal differentiation of embryonal carcinoma P19 cells in the absence of retinoic acid. *Cell Mol Neurobiol* 24:343–356

- Kim SU, Park IH, Kim TH, Kim KS, Choi HB, Hong SH, Bang JH, Lee MA, Joo IS, Lee CS, Kim YS (2006) Brain transplantation of human neural stem cells transduced with tyrosine hydroxylase and GTP cyclohydrolase 1 provides functional improvement in animal models of Parkinson disease. *Neuropathology* 26:129–140
- Lum M, Turbic A, Mitrovic B, Turnley AM (2009) Fibroblast growth factor-9 inhibits astrocyte differentiation of adult mouse neural progenitor cells. *J Neurosci Res* 87:2201–2210
- Ma Q, Fode C, Guillemot F, Anderson DJ (1999) Neurogenin1 and neurogenin2 control two distinct waves of neurogenesis in developing dorsal root ganglia. *Genes Dev* 13:1717–1728
- May R, Sureban SM, Hoang N, Riehl TE, Lightfoot SA, Ramanujam R, Wyche JH, Anant S, Houchen CW (2009) DCAMKL-1 and LGR5 mark quiescent and cycling intestinal stem cells respectively. *Stem Cells*. doi:10.1002/stem.193
- Morita H, Mazerbourg S, Bouley DM, Luo CW, Kawamura K, Kuwabara Y, Baribault H, Tian H, Hsueh AJ (2004) Neonatal lethality of LGR5 null mice is associated with ankyloglossia and gastrointestinal distension. *Mol Cell Biol* 24:9736–9743
- Morrison SJ (2001) Neuronal differentiation: proneural genes inhibit gliogenesis. *Curr Biol* 11:R349–R351
- Niida A, Hiroko T, Kasai M, Furukawa Y, Nakamura Y, Suzuki Y, Sugano S, Akiyama T (2004) DKK1, a negative regulator of Wnt signaling, is a target of the β -catenin/TCF pathway. *Oncogene* 23:8520–8526
- Obayashi S, Tabunoki H, Kim SU, Satoh J (2009) Gene expression profiling of human neural progenitor cells following the serum-induced astrocyte differentiation. *Cell Mol Neurobiol* 29:423–438
- Ootani A, Li X, Sangiorgi E, Ho QT, Ueno H, Toda S, Sugihara H, Fujimoto K, Weissman IL, Capecchi MR, Kuo CJ (2009) Sustained in vitro intestinal epithelial culture within a Wnt-dependent stem cell niche. *Nat Med* 15:701–706
- Ota M, Ito K (2003) Induction of neurogenin-1 expression by sonic hedgehog: its role in development of trigeminal sensory neurons. *Dev Dyn* 227:544–551
- Prakash N, Wurst W (2007) A Wnt signal regulates stem cell fate and differentiation in vivo. *Neurodegener Dis* 4:333–338
- Sato H, Ishida S, Toda K, Matsuda R, Hayashi Y, Shigetaka M, Fukuda M, Wakamatsu Y, Itai A (2005) New approaches to mechanism analysis for drug discovery using DNA microarray data combined with KeyMolnet. *Curr Drug Discov Technol* 2:89–98
- Sato T, Vries RG, Snippert HJ, van de Wetering M, Barker N, Stange DE, van Es JH, Abo A, Kujala P, Peters PJ, Clevers H (2009) Single Lgr5 stem cells build crypt-villus structures in vitro without a mesenchymal niche. *Nature* 459:262–265
- Sommer L, Ma Q, Anderson DJ (1996) Neurogenins, a novel family of atonal-related bHLH transcription factors, are putative mammalian neuronal determination genes that reveal progenitor cell heterogeneity in the developing CNS and PNS. *Mol Cell Neurosci* 8:221–241
- Sun Y, Nadal-Vicens M, Misono S, Lin MZ, Zubiaga A, Hua X, Fan G, Greenberg ME (2001) Neurogenin promotes neurogenesis and inhibits glial differentiation by independent mechanisms. *Cell* 104:365–376
- Tanese K, Fukuma M, Yamada T, Mori T, Yoshikawa T, Watanabe W, Ishiko A, Amagai M, Nishikawa T, Sakamoto M (2008) G-protein-coupled receptor GPR49 is up-regulated in basal cell carcinoma and promotes cell proliferation and tumor formation. *Am J Pathol* 173:835–843
- Wu B, Crompton SP, Hughes CC (2007) Wnt signaling induces matrix metalloproteinase expression and regulates T cell transmigration. *Immunity* 26:227–239
- Yamamoto Y, Sakamoto M, Fujii G, Tsuiji H, Kenetaka K, Asaka M, Hirohashi S (2003) Overexpression of orphan G-protein-coupled receptor, Gpr49, in human hepatocellular carcinomas with β -catenin mutations. *Hepatology* 37:528–533

2 **TDP-43 Dimerizes in Human Cells in Culture**

3 Yuki Shiina · Kunimasa Arima ·
4 Hiroko Tabunoki · Jun-ichi Satoh

5 Received: 8 October 2009 / Accepted: 16 December 2009
6 © Springer Science+Business Media, LLC 2009

7 **Abstract** TAR DNA-binding protein-43 (TDP-43) is
8 a 43-kDa nuclear protein involved in regulation of
9 gene expression. Abnormally, phosphorylated, ubiquiti-
10 nated, and aggregated TDP-43 constitute a principal
11 component of neuronal and glial cytoplasmic and nuclear
12 inclusions in the brains of frontotemporal lobar degener-
13 ation with ubiquitin-positive inclusions (FTLD-U) and
14 amyotrophic lateral sclerosis (ALS), although the molec-
15 ular mechanism that triggers aggregate formation remains
16 unknown. By Western blot analysis using anti-TDP-43
17 antibodies, we identified a band with an apparent molec-
18 ular mass of 86 kDa in HEK293, HeLa, and SK-N-SH
19 cells in culture. It was labeled with both N-terminal-
20 specific and C-terminal-specific TDP-43 antibodies, en-
21 riched in the cytosolic fraction, and the expression levels
22 were reduced by TDP-43 siRNA but unaltered by treat-
23 ment with MG-132 or by expression of ubiquilin-1 or
24 casein kinase-1. By immunoprecipitation analysis, we
25 found the interaction between the endogenous full-length
26 TDP-43 and the exogenous Flag-tagged TDP-43, and
27 identified the N-terminal half of TDP-43 spanning amino
28 acid residues 3–183 as an intermolecular interaction
29 domain. When the tagged 86-kDa tandemly connected
30 dimer of TDP-43 was overexpressed in HEK293, it was
31 sequestered in the cytoplasm and promoted an accumu-
32 lation of high-molecular-mass TDP-43-immunoreactive

proteins. Furthermore, the 86-kDa band was identified in
the immunoblot of human brain tissues, including those of
ALS. These results suggest that the 86-kDa band repre-
sents dimerized TDP-43 expressed constitutively in nor-
mal cells under physiological conditions.

Keywords Dimerization · Immunoprecipitation ·
Seed · TDP-43

Abbreviations

TDP-43	TAR DNA-binding protein-43	41
FTLD-U	Frontotemporal lobar degeneration with ubiquitin-positive inclusions	42
ALS	Amyotrophic lateral sclerosis	43
RRM	RNA-recognition motif	44
CSNK1A1	Casein kinase-1 alpha-1	45
UBQLN1	Ubiquilin-1	46
PARP	PolyADP ribose-polymerase	47

Introduction

TAR DNA-binding protein-43 (TDP-43) is a 43-kDa
nuclear protein encoded by the TARDBP gene on chro-
mosome 1p36.22, originally identified as a transcriptional
repressor of the human immunodeficiency virus (HIV)
gene (Ou et al. 1995). TDP-43, capable of interacting with
UG and TG repeat stretches of RNA and DNA (Buratti and
Baralle 2008). It plays a role in regulation of exon exclu-
sion and inclusion of target genes during alternative
splicing events, thereby being involved in cell division,
apoptosis, mRNA stability, and microRNA biogenesis
(Wang et al. 2008). TDP-43 is highly conserved through

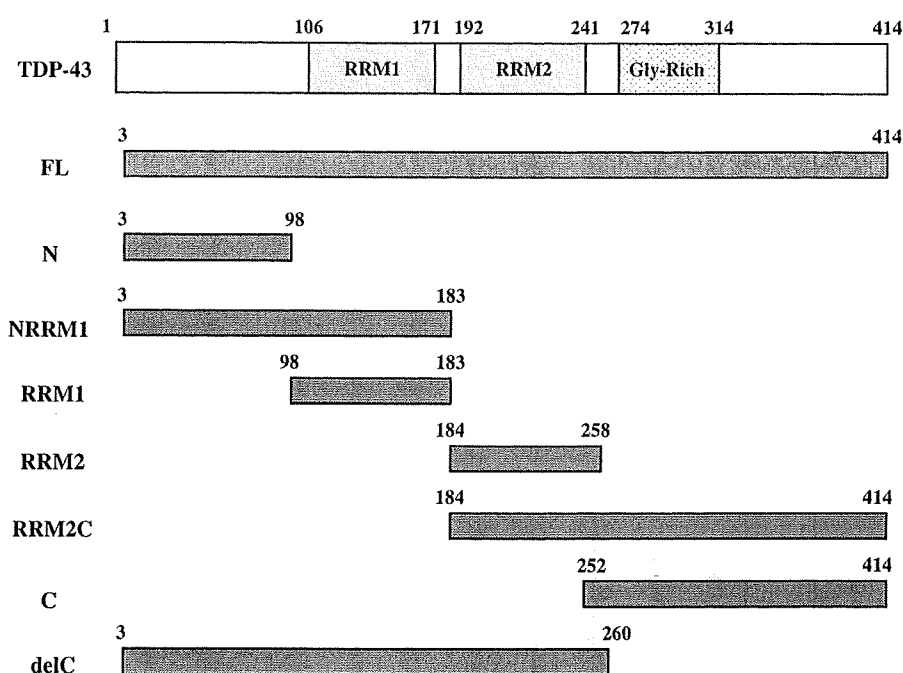
A1 Y. Shiina · H. Tabunoki · J. Satoh (✉)
A2 Department of Bioinformatics and Molecular Neuropathology,
A3 Meiji Pharmaceutical University, 2-522-1 Noshio Kiyose,
A4 Tokyo 204-8588, Japan
A5 e-mail: satoj@my-pharm.ac.jp

A6 K. Arima
A7 Department of Psychiatry, National Center Hospital, National
A8 Center of Neurology and Psychiatry, Tokyo 187-8551, Japan

63	evolution from human to <i>Caenorhabditis elegans</i> , sug-	116
64	gesting a phylogenetically pivotal role (Ayala et al. 2005).	117
65	In its protein structure, TDP-43 is composed of an N-ter-	118
66	terminal domain and two highly conserved RNA-recognition	119
67	motifs named RRM1 and RRM2, followed by a glycine-	120
68	rich C-terminal domain that mediates the interaction of	121
69	TDP-43 with heterogeneous ribonucleoproteins (Buratti	122
70	and Baralle 2008; Wang et al. 2008). The RRM1 domain is	123
71	necessary and sufficient for recognition of UG and TG	
72	repeat stretches of nucleic acids, while the C-terminal	
73	domain plays an essential role in regulation of splicing	
74	(Ayala et al. 2005; Buratti et al. 2005). In normal cells	
75	under physiological conditions, more than 90% of total	
76	TDP-43 proteins are accumulated in the nucleus, enriched	
77	in nuclear bodies, where TDP-43 coexists with survival	
78	motor neuron (SMN) and fragile X mental retardation	
79	(FMR) proteins, whereas very small amounts are located in	
80	the cytoplasm (Wang et al. 2008).	
81	Abnormally, phosphorylated and ubiquitinated TDP-43	
82	constitutes a principal component of neuronal cytoplasmic	
83	inclusions (NCIs), dystrophic neurites (DNs), neuronal	
84	intranuclear inclusions (NIIs), and glial cytoplasmic	
85	inclusions (GCIs), in the brains of frontotemporal lobar	
86	degeneration with ubiquitin-positive inclusions (FTLD-U)	
87	and amyotrophic lateral sclerosis (ALS) (Arai et al. 2006;	
88	Neumann et al. 2006). In view of overlapping clinico-	
89	pathological features, both FTLD-U and ALS are	
90	categorized into a novel disease entity named TDP-43	
91	proteinopathy (Geser et al. 2009). In TDP-43 proteinopa-	
92	thy, TDP-43 protein often translocates from the nucleus to	
93	the cytoplasm by forming detergent-insoluble urea-soluble	
94	aggregates, where it is hyperphosphorylated, polyubiquiti-	
95	nated, and proteolytically cleaved to produce 25- and	
96	35-kDa C-terminal fragments (Neumann et al. 2006; Zhang	
97	et al. 2007; Hasegawa et al. 2008). Furthermore, abnormal	
98	TDP-43 immunoreactivity is occasionally found in the	
99	brains of Alzheimer disease (AD), dementia with Lewy	
100	bodies (DLB), Pick disease (PiD), corticobasal degenera-	
101	tion (CBD), argyrophilic grain disease (AGD), the Guam	
102	parkinsonism-dementia complex (G-PDC), and Huntington	
103	disease (HD) (Geser et al. 2009). The C-terminal domain of	
104	TDP-43 contains multiple phosphorylation consensus sites,	
105	among which the major phosphorylated epitopes are cre-	
106	ated by casein kinase-1 (CK1) (Kametani et al. 2009). Out	
107	of them, phosphorylation of Ser409/410 on TDP-43 is the	
108	pathological hallmark of certain sporadic and familial ALS	
109	cases (Neumann et al. 2009). Hyperphosphorylation of	
110	TDP-43 promotes oligomerization and fibril formation in	
111	vitro (Hasegawa et al. 2008). Importantly, missense	
112	mutations expressing mutant proteins with an increased	
113	aggregation property are clustered in the C-terminal	
114	domain of the TDP-43 gene in the patients with sporadic	
115	and familial ALS (Kabashi et al. 2008).	
	At present, the precise molecular events that trigger	116
	aggregate formation of TDP-43 remain to be characterized.	117
	In this study, by Western blot analysis, we identified a	118
	small amount of the TDP-43-immunoreactive 86-kDa	119
	protein constitutively expressed in HEK293, HeLa, and	120
	SK-N-SH cells in culture and human brain tissues in vivo.	121
	We suppose that this 86-kDa protein represents dimerized	122
	TDP-43.	123
	Methods	124
	Human Cell Lines and Brain Tissues	125
	Human cell lines, such as SK-N-SH neuroblastoma, HeLa	126
	cervical carcinoma, and HEK293 embryonic kidney cells,	127
	were maintained in the culture medium consisting of	128
	DMEM (Invitrogen, Carlsbad, CA) supplemented with	129
	10% fetal bovine serum (FBS), 100-U/ml penicillin, and	130
	100- μ g/ml streptomycin. In some experiments, the cells	131
	were exposed for 24 h to 1- μ M MG-132 (Calbiochem, San	132
	Diego, CA), a proteasome inhibitor. Human brain tissues of	133
	the cerebrum (CBR) and the cerebellum (CBL) were pro-	134
	vided by Research Resource Network (RRN), Japan. They	135
	include a 29-year-old woman with secondary progressive	136
	MS (MS#1), a 40-year-old woman with secondary pro-	137
	gressive MS (MS#2), a 43-year-old woman with primary	138
	progressive MS (MS#3), a 76-year-old woman with PD	139
	(PD#1), a 61-year-old woman with ALS (ALS#1), a 74-	140
	year-old woman with ALS (ALS#2), a 61-year-old man	141
	with ALS (ALS#3), a 66-year-old man with ALS (ALS#4),	142
	a 73-year-old man with schizophrenia (SCH#1), and a 77-	143
	year-old woman with depression (DEP#1). The post-	144
	mortem interval of the cases ranges from 1.5 to 10 h prior	145
	to freezing the brain tissues. All autopsies were performed	146
	at the National Center Hospital, National Center of Neu-	147
	rology and Psychiatry (NCNP), Tokyo, Japan. This study	148
	was approved by the Ethics Committee of NCNP. Written	149
	informed consent was obtained from all the autopsy cases	150
	examined.	151
	Western Blot Analysis	152
	To prepare total protein extract, the cells and tissues were	153
	homogenized in either M-PER protein extraction buffer	154
	(Pierce, Rockford, IL) or RIPA buffer (Sigma, St. Louis,	155
	MO), supplemented with a cocktail of protease inhibitors	156
	(Sigma). The cell and tissue lysate were centrifuged at	157
	12,000 rpm for 5 min at room temperature (RT). The	158
	mixture of the supernatant and a $\times 2$ Lammeli loading	159
	buffer was boiled and separated on a 10 or 12% SDS-PAGE	160
	gel. The molecular weight of the proteins was calculated by	161
	the position of a broad-range SDS-PAGE standard	162

- 163 (BioRad, Hercules, CA). The protein concentration was
164 determined by a Bradford assay kit (BioRad). After gel
165 electrophoresis, the protein was transferred onto nitrocel-
166 lulose membranes, and immunolabeled at RT overnight
167 with rabbit polyclonal anti-TDP-43 antibody that recog-
168 nizes amino acid residues 1–260 located at the N-terminal
169 half of the human TDP-43 protein (1:10,000; 10782-2-AP;
170 Proteintech Group, Chicago, IL) or rabbit polyclonal anti-
171 TDP-43 antibody that recognizes amino acid residues 350–
172 414 located at the C-terminus of the human TDP-43 protein
173 (1:500; NB110-55376; Novus Biologicals, Littleton, CO).
174 Then, the membranes were incubated at RT for 30 min with
175 HRP-conjugated anti-rabbit IgG (Santa Cruz Biotechnol-
176 ogy, Santa Cruz, CA). The specific reaction was visualized
177 by exposing the membranes to a chemiluminescent sub-
178 strate (Pierce). In some experiments, the antibodies were
179 stripped by incubating the membranes at 50°C for 30 min in
180 stripping buffer, composed of 62.5-mM Tris-HCl, pH
181 6.7, 2% SDS, and 100-mM 2-mercaptoethanol. Then, the
182 membranes were processed for relabeling with mouse
183 monoclonal anti-ubiquitin antibody (P4D1; Santa Cruz
184 Biotechnology), rabbit polyclonal anti-polyADP ribose-
185 polymerase (PARP) antibody (Roche Diagnostics, Tokyo,
186 Japan), rabbit anti-Halo tag antibody (Promega, Madison,
187 WI), goat polyclonal anti-HSP60 antibody (N-20; Santa
188 Cruz Biotechnology) for an internal control of protein
189 loading, anti-Xpress antibody (Invitrogen), or anti-V5
190 antibody (Invitrogen).
- 191 **Fractionation of Cellular Proteins**
- 192 To determine subcellular location of dimeric TDP-43
193 proteins, we performed the differential extraction of native
194 proteins using the ProteoExtract subcellular Proteome
195 Extraction kit (Calbiochem, San Diego, CA). Then, the
196 fractionated proteins from cytosol, membrane, nuclear, and
197 cytoskeletal compartments were processed for Western
198 blot with anti-TDP-43 antibody (10782-2-AP). The blots
199 were relabeled with goat polyclonal anti-HSC70 antibody
200 (K19; Santa Cruz Biotechnology), rabbit polyclonal
201 anti-pan-cadherin antibody (RB-9036; Thermo Fisher
202 Scientific, Fremont, CA), mouse monoclonal anti-vimentin
203 antibody (V9; Santa Cruz Biotechnology), and mouse
204 monoclonal anti-histone H1 antibody (SPM256; AnaSpec,
205 San Jose, CA).
- 206 **Vector Construction**
- 207 To study the molecular interaction between TDP-43 pro-
208 teins, the genes coding for the full-length (FL) TDP-43
209 (GenBank Accession No. NM_007375) and a panel of
210 truncated forms of TDP43 (Fig. 1) or GFP were amplified
211 by PCR using PfuTurbo DNA polymerase (Stratagene,
La Jolla, CA) and the sense and the antisense primer sets
listed in Table 1. After digesting the PCR products with
restriction enzymes KpnI, XbaI, XhoI, and NotI (New
England BioLabs, Beverly, MA), they were cloned in the
expression vector p3XFLAG-CMV7.1 (Sigma), pFN21A-
CMV Flexi (Promega), or pCMV-Myc (Clontech, Moun-
tain View, CA) to express a fusion protein with an
N-terminal Flag, Halo, or Myc tag. The vector containing
the tandemly-connected dimer of TDP-43, tentatively
named as TDP-43 tandem dimer, was constructed by tail-
to-head ligation of two TDP-43 PCR products with distinct
restriction-enzyme-digested ends, one having a C-terminal
KpnI site and the other having an N-terminal KpnI site
(Table 1). The siRNA vector constructs targeted to TDP-43
and a scrambled sequence (Table 1) were generated using
GeneClip U1 Hairpin cloning system (Promega) following
the manufacturer's instruction.
- To investigate the role of casein kinase-1 alpha-1
(CSNK1A1) and ubiquitin-1 (UBQLN1) in dimer formation
of TDP-43, the genes coding for CSNK1A1 (NM_001892),
and UBQLN1 (NM_013438), were amplified by PCR using
PfuTurbo DNA polymerase and the sense and the antisense
primer sets listed in Table 1. Then, the PCR products were
cloned in the expression vector pEF6/V5/His-TOPO
(Invitrogen) or pCDNA4/HisMax-TOPO (Invitrogen) to
express a fusion protein with a C-terminal V5 tag or an
N-terminal Xpress tag.
- All the vectors were transfected in the cells using
Lipofectamine 2000 reagent (Invitrogen).
- Immunoprecipitation**
- Immunoprecipitation analysis was performed according to
the methods described previously (Sato et al. 2009).
24–48 h after transfection of the vectors, HEK293 cells were
homogenized in M-PER protein extraction buffer supple-
mented with a cocktail of protease inhibitors (Sigma). The
protein extract was incubated at 4°C overnight with mouse
monoclonal anti-Flag M2 affinity gel (Sigma). After several
washes, the anti-Flag M2 affinity gel-binding proteins were
eluted by incubating the gel with an exceeding amount of
Flag peptide (Sigma). Then, the eluted proteins were pre-
cipitated by cold acetone. The immunoprecipitates were
processed for Western blot with mouse monoclonal anti-
Flag M2 antibody (Sigma) or rabbit polyclonal anti-TDP-43
antibody (10782-2-AP). Reciprocal coimmunoprecipitation
analysis was performed according to the methods described
previously (Sato et al. 2009).
- Cell Imaging**
- To visualize the subcellular location of TDP-43 in cultured
cells, the genes encoding the monomer or the tandem dimer

Fig. 1 The structural domains of the human TDP-43 protein. The domain structure of the human TDP-43 protein is shown on the top with the position of amino acid residues. The genes encoding the full-length (FL) TDP-43 protein and a panel of truncated forms, such as the C-terminal domain-cleaved protein (*delC*), the C-terminal domain fragment (C), the N-terminal domain fragment (N), RRM1, RRM2, the N-terminal domain plus RRM1 (NRRM1), and the C-terminal domain plus RRM2 (RRM2C), were cloned in the expression vectors as listed in Table 1



261 of TDP-43 were cloned in the vector pFN21A-CMV
 262 Flexi (Table 1), and transfected in HEK293 cells. 24 h
 263 after transfection, the live cells were exposed for 15 min to
 264 Oregon Green (Promega), a fluorochrome specifically
 265 bound to the Halo tag protein, fixed in 4% paraformaldehyde,
 266 and exposed to 4',6'-diamidino-2-phenylindole
 267 (DAPI). They were mounted with glycerol-polyvinyl
 268 alcohol and examined under the Olympus BX51 universal
 269 microscope.

270 Results

271 Constitutive Expression of TDP-43 Dimer in Human 272 Cell Cultures

273 By Western blot of the detergent-soluble protein extract
 274 with anti-TDP-43 antibody (10782-2-AP), HEK293, HeLa,
 275 and SK-N-SH cells in culture expressed constitutively a
 276 major 43-kDa protein representing the full-length (FL)
 277 TDP-43 protein, variable levels of 36- and 27-kDa proteins
 278 representing the N-terminally cleaved fragments, and a
 279 small but discernible amount of the 86-kDa protein (Fig. 2,
 280 panels a-c, lane 1). By densitometric analysis, the 86-kDa
 281 protein consisted of approximately 4% of total TDP-43-
 282 immunoreactive proteins in HEK293 cells, where mini-
 283 mum 50 µg of protein is required for loading on the gel to
 284 detect the 86-kDa protein. A 24-h treatment of the cells
 285 with MG-132, an inhibitor of proteasome function, did not
 286 alter the expression levels of the 86-kDa protein (Fig. 2,
 287 panels a-c, lane 2).

288 Because the 86-kDa TDP-43-immunoreactive protein
 289 has not been reported previously, we assumed that it rep-
 290 represents a fairly small fraction of the endogenous FL TDP-
 291 43 dimer, based on its molecular weight. First, to charac-
 292 terize this protein, we concentrated both 86- and 43-kDa
 293 proteins extracted from the corresponding SDS-PAGE gel
 294 bands. They were then processed for Western blot analysis
 295 using anti-TDP-43 antibody (10782-2-AP) that reacts with
 296 amino acid residues 1-260 located at the N-terminal half or
 297 anti-TDP-43 antibody (NB110-55376) that reacts with
 298 amino acid residues 350-414 located at the C-terminus of
 299 the human TDP-43 protein. Both antibodies recognized the
 300 86-kDa protein, along with the 43-kDa protein (Fig. 3A,
 301 panels a and b, lanes 1 and 2). In contrast, the exclusion of
 302 the primary antibodies did not react with either (Fig. 3A,
 303 panel c, lanes 1 and 2). These results argue against the
 304 possibility that the 86-kDa protein reflects a protein of non-
 305 TDP43 origin that simply exhibits cross-reactivity to TDP-
 306 43 on the blot. Furthermore, transient expression of the
 307 siRNA vector targeted specifically to TDP-43 but not to a
 308 scrambled sequence substantially reduced the expression of
 309 both 43- and 86-kDa TDP-43 immunoreactive proteins,
 310 suggesting that the 86-kDa protein is composed of TDP-43
 311 (Fig. 3B, panels a and b, lanes 2 and 3).

312 Overexpression of ubiquilin-1 (UBQLN1), a proteasome-
 313 targeting factor that promotes the formation of cytoplasmic
 314 aggregations of TDP-43 (Kim et al. 2008) or casein kinase-
 315 1 alpha-1 (CSNK1A1), a protein kinase that mediates
 316 phosphorylation of major serine epitopes in the C-terminal
 317 domain of TDP-43 (Kametani et al. 2009), did not change
 318 the levels of expression of the 86-kDa protein in HEK293

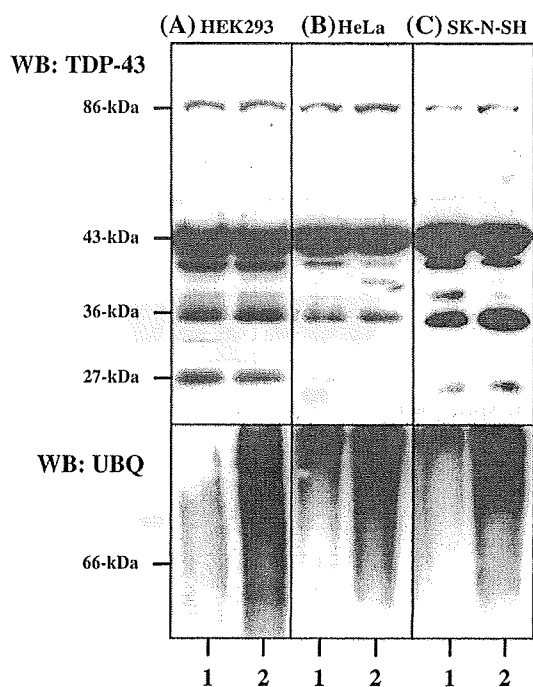


Fig. 2 The constitutive expression of an 86-kDa TDP-43-immunoreactive protein in human cell lines in culture. The detergent-soluble protein extract of HEK293, HeLa, and SK-N-SH cells exposed for 24 h to the vehicle (dimethylsulfoxide) (lane 1) or 1- μ M MG-132 (lane 2) was processed for Western blot with anti-TDP43 antibody (upper panels) or with anti-ubiquitin antibody (lower panels). A small but discernible amount of the 86-kDa TDP-43-immunoreactive band is expressed in all the cells examined

319 cells (Fig. 3C, upper panel a, lane 3; upper panel b, lane 6).
 320 Furthermore, either a 48-h exposure of the cells to 10-nM
 321 okadaic acid, an inhibitor of protein phosphatases 1 and
 322 2A, or a 48-h treatment with 20- μ M hydrogen peroxide, an
 323 oxidative stress inducer did not alter the levels of expres-
 324 sion of the 86-kDa protein (not shown). The use of dif-
 325 ferent extraction buffers, either the M-PER protein
 326 extraction buffer or the RIPA buffer for protein extraction
 327 or the inclusion of 20-mM dithiothreitol (DTT) or an
 328 increased amount of 2-mercaptoethanol (2-ME) that redu-
 329 ces a typical disulfide bond in the sample-loading buffer
 330 did not affect the levels of expression of the 86-kDa pro-
 331 tein, suggesting that the intermolecular interaction is fairly
 332 a detergent-resistant (not shown).

333 Next, we conducted immunoprecipitation analysis. After
 334 Flag-tagged FL TDP-43 or Flag-tagged GFP was expressed
 335 in HEK293, HeLa, and SK-N-SH cells, the protein extract
 336 was processed for immunoprecipitation with anti-Flag
 337 affinity gel. Then, the precipitates were eluted and pro-
 338 cessed for Western blot with anti-TDP-43 antibody (10782-
 339 2-AP). The proteins binding to Flag-tagged TDP-43 always
 340 included the endogenous FL TDP-43 protein in addition to
 341 several truncated species (Fig. 4A, upper panels a-c, lane
 342 1). We identified multimeric forms of Flag-tagged TDP-43

343 proteins, when the immunoprecipitates were overloaded on
 344 the gel (Fig. 4B, lanes 1 and 2). In contrast, the precipitates
 345 of Flag-tagged GFP-binding proteins were completely
 346 devoid of the endogenous TDP-43 protein (Fig. 4A, upper
 347 panels a-c, lane 2). Furthermore, reciprocal immunopre-
 348 cipitation analysis verified that Flag-tagged TDP-43 inter-
 349 acts with Myc-tagged TDP-43, excluding non-specific
 350 binding of TDP-43 to immunoglobulins (Fig. 4C, upper
 351 and lower panels, lanes 1-3). These results indicate that a
 352 substantial part of endogenous TDP-43 protein interacts
 353 with the exogenous Flag-tagged TDP-43 but not with the
 354 exogenous Flag-tagged GFP, suggesting that TDP-43
 355 intrinsically forms the dimer, and TDP-43 forms a specific
 356 molecular interaction with TDP-43. Taken all these results
 357 together, we concluded that the 86-kDa protein represents a
 358 dimer of TDP-43.

359 By fractionation analysis of total cellular proteins of
 360 HEK293, the 86-kDa protein was highly enriched in the
 361 cytosolic fraction but absent in the nuclear fraction, while the
 362 43-kDa FL endogenous TDP-43 protein was distributed in all
 363 the compartments, including cytosol, membrane, nuclear,
 364 and cytoskeletal fractions (Fig. 5, panel a, lanes 1-5).

Involvement of N-Terminal Half in Intermolecular Interaction of TDP-43 Proteins

365 To identify the domains involved in the intermolecular
 366 interaction of TDP43 proteins, a panel of Flag-tagged
 367 truncated proteins (Fig. 1), including the C-terminal frag-
 368 ment spanning amino acid residues 252-414 (C), the
 369 N-terminal fragment spanning amino acid residues 3-98
 370 (N), the RRM1 domain spanning amino acid residues 98-
 371 183 (RRM1), the RRM2 domain spanning amino acid
 372 residues 184-258 (RRM2), the N-terminal domain plus
 373 RRM1 spanning amino acid residues 3-183 (NRRM1), the
 374 C-terminal domain plus RRM2 spanning amino acid resi-
 375 dues 184-414 (RRM2C), and the C-terminal domain-
 376 cleaved protein spanning amino acid residues 3-260 (delC)
 377 were individually expressed in HEK293 cells. Then, the
 378 protein extract was processed for immunoprecipitation
 379 with anti-Flag affinity gel, followed by Western blot with
 380 anti-TDP-43 antibody (10782-2-AP). The anti-TDP-43
 381 antibody (10782-2-AP) reacted with FL TDP-43, delC, N,
 382 NRRM1, RRM2, and RRM2C, but not with RRM1 or C
 383 (Fig. 6, lanes 1, 3, 5, 9, 11, and 15). These results indicate
 384 that the 10782-2-AP antibody recognizes at least two
 385 separate epitopes located in N and RRM2 in the N-terminal
 386 half of TDP-43. After immunoprecipitation, the endoge-
 387 nous FL TDP-43 protein was detected exclusively in the
 388 precipitates of Flag-tagged FL TDP-43, delC, and NRRM1
 389 fragments (Fig. 6, lanes 1, 3, and 9). These results
 390 suggest that the continuous N-terminal half domain
 391 spanning amino acid residues 3-183, possibly by
 392
 393

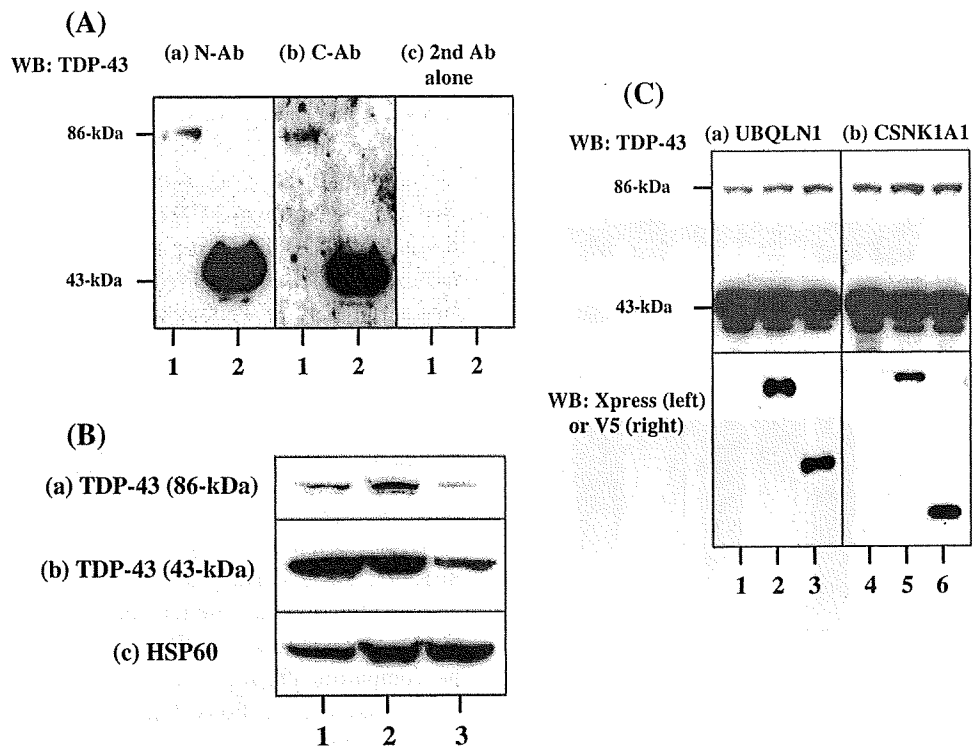


Fig. 3 The characterization of the 86-kDa protein. **A** The immunoblotting of the protein with N- or C-terminal-specific anti-TDP-43 antibodies. Both 86- and 43-kDa proteins were extracted from the corresponding SDS-PAGE gel bands, concentrated, and processed for Western blot with the N-terminal-specific anti-TDP-43 antibody (*panel a*), the C-terminal-specific anti-TDP-43 antibody (*panel b*), or the secondary antibody alone (*panel c*). The lanes (1 and 2) represent the 86- and the 43-kDa protein, respectively. **B** The effects of transient expression of TDP-43 siRNA. SK-N-SH cells were transfected with the siRNA expression vector targeted to TDP-43 or a scrambled sequence listed in Table 1. 96 h after transfection, the protein extract was processed for Western blot with anti-TDP-43

antibody (*panels a and b*) or anti-HSP60 antibody, an internal control for protein loading (*panel c*). The lanes (1–3) represent non-transfected cells, the cells transfected with the vector of a scrambled sequence, and the cells transfected with the vector of TDP-43 siRNA, respectively. **C** The effects of expression of ubiquitin-1 (UBQLN1) and casein kinase-1 alpha-1 (CSNK1A1). HEK293 cells were untransfected (*lanes 1 and 4*) or transfected with the expression vectors of Xpress-tagged LacZ (*lane 2*), Xpress-tagged UBQLN1 (*lane 3*), V5-tagged LacZ (*lane 5*), or V5-tagged CSNK1A1 (*lane 6*). The detergent-soluble protein extract was processed for Western blot with anti-TDP-43 antibody (*upper panels*), anti-Xpress antibody (*the left lower panel*), or anti-V5 antibody (*the right lower panel*)

394 constructing a conformationally ordered interacting
395 domain, but neither N nor RRM1 alone, is sufficient for the
396 intermolecular interaction of TDP-43, while the C-terminal
397 domain is dispensable for this.

398 TDP-43 Dimer Acts as a Seed for Promoting
399 Aggregation of TDP-43 Proteins

400 To investigate a role of the TDP-43 dimer in TDP-43 protein
401 aggregation, Halo-tagged TDP-43 FL monomer, tandem
402 dimer, or GFP was expressed in HEK293 cells. Then, the
403 blot was labeled with anti-TDP43 antibody (10782-2-AP),
404 anti-Halo tag antibody, anti-PARP antibody, anti-ubiquitin
405 antibody, or anti-HSP60 antibody. The expression of the
406 TDP-43 tandem dimer but neither the monomer nor GFP
407 greatly enhanced an accumulation of TDP-43-immunore-
408 active proteins with higher molecular mass ranging from
409 70- to 200-kDa (Fig. 7A, panel a, lane 5), while the levels of

expression of Halo-tagged proteins were identical among 410
GFP, the monomer, and the dimer (Fig. 7A, panel b, lanes 411
3–5). These results suggest that TDP-43 dimer by acting as a 412
seed promotes protein aggregation that involves various 413
endogenous species of TDP-43, including N-termi- 414
nally cleaved fragments. Unexpectedly, untransfected and 415
untreated HEK293 cells expressed constitutively both unc- 416
leaved (116-kDa) and cleaved (85-kDa) forms of PARP 417
without morphological features of apoptosis (Fig. 7A, panel 418
c, lanes 1–5). The expression of TDP-43 tandem dimer did 419
not alter the levels of the cleaved PARP (Fig. 7A, panel c, 420
lane 5) or did not elevate substantially the levels of ubiqui- 421
tinated proteins, compared with the cells with expression of 422
GFP or the monomer (Fig. 7A, panel d, lanes 3–5). In con- 423
trast, a 24-h treatment with MG-132 enhanced an accumu- 424
lation of ubiquitinated proteins (Fig. 7A, panel d, lane 2). 425
Importantly, the numbers of the cells presenting with 426
nuclear accumulation of Halo tag immunoreactivity was 427

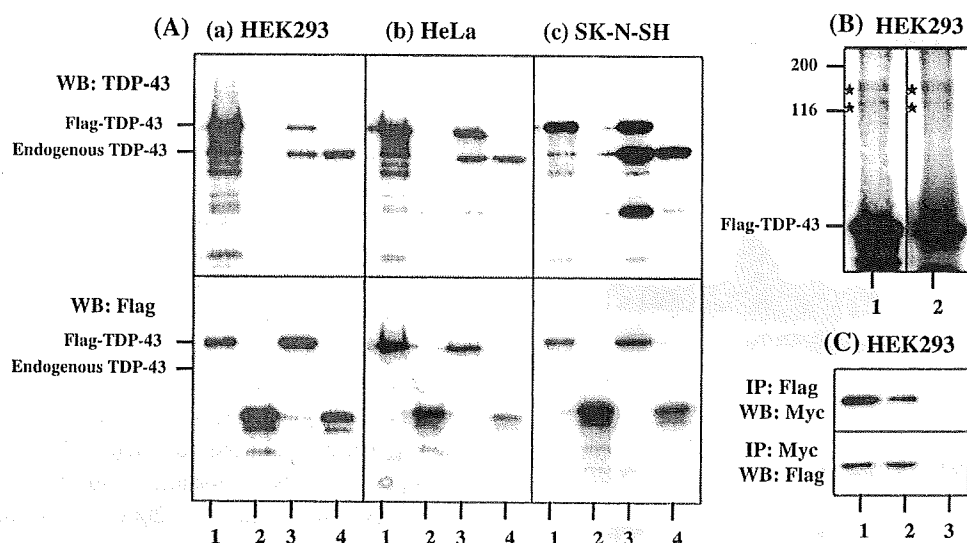


Fig. 4 Immunoprecipitation analysis of Flag-tagged TDP-43-binding proteins. **A** Coimmunoprecipitation with Flag-tagged proteins. Flag-tagged FL TDP-43 (lanes 1 and 3) or GFP (lanes 2 and 4) was expressed in HEK293 (panel a), HeLa (panel b), and SK-N-SH (panel c) cells. The detergent-soluble protein extract was processed for immunoprecipitation (IP) with anti-Flag M2 affinity gel, followed by Western blot (WB) with anti-TDP-43 antibody (upper panels) or anti-Flag M2 antibody (lower panels). The lanes (1–4) represent (1 and 2) the immunoprecipitates and (3 and 4) the corresponding input controls. **B** Flag-tagged TDP-43 constitutes multimeric forms. Flag-tagged FL TDP-43 was expressed in HEK293 cells, and then

processed for IP with anti-Flag M2 affinity gel, followed by WB with anti-TDP-43 antibody or anti-Flag M2 antibody. Immunoprecipitates were overloaded on a 10% SDS-PAGE gel. The lanes (1, 2) represent anti-TDP-43 antibody and anti-Flag M2 antibody, respectively. Multimeric forms are indicated by stars. **C** Reciprocal coimmunoprecipitation analysis. Flag-tagged FL TDP-43 and Myc-tagged FL TDP-43 were coexpressed in HEK293. IP followed by WB was performed using the antibody against Myc (upper panel) or Flag (lower panel), reciprocally. The lanes (1–3) represent input control, IP with anti-Flag M2 or anti-Myc antibody, and IP with normal mouse or rabbit IgG, respectively

428 significantly smaller in the tandem dimer-expressing
429 HEK293 cells than those expressing the monomer ($P =$
430 0.00008, two-tailed Student's *t* test) (Fig. 7B, panels a–d and
431 Fig. 7C).

432 Identification of TDP-43 Dimer in Human Brain 433 Tissues

434 Finally, we conducted Western blot analysis of the deter-
435 gent-soluble protein extract of human brain tissues with
436 anti-TDP43 antibody (10782-2-AP). The expression of the
437 86-kDa TDP-43 dimer, along with the 43-kDa FL TDP-43
438 monomer and several cleaved fragments, was identified at
439 varying levels in both the cerebrum (CBR) and the cere-
440 bellum (CBL) of the patients with PD, ALS, MS, schizo-
441 phrenia, or depression (Fig. 8, panel a, lanes 1–15).
442 Although the brain tissues derived from ALS patients
443 constantly expressed higher levels of the TDP-43 dimer,
444 we could not obtain the definite conclusion because of the
445 limitation of the samples examined.

446 Discussion

447 By Western blot analysis, we identified the expression of
448 the 86-kDa TDP-43-immunoreactive protein in HEK293,

HeLa, and SK-N-SH cells in culture. We considered this 449
protein as a dimer of TDP-43 for the following reasons. 450
First, the molecular weight of the protein corresponds 451
exactly to that of the dimer. Second, two different anti- 452
TDP-43 antibodies that recognize distinct antigenic epi- 453
topes located in the N- or the C-terminal domain equally 454
labeled the 86-kDa protein, excluding the possibility of 455
immunological cross reactivity on a non-TDP-43 protein. 456
Third, the levels of expression of the 86-kDa protein 457
were greatly reduced by treatment with TDP-43 siRNA, 458
suggesting that it is composed of TDP-43. Fourth, by 459
immunoprecipitation analysis, we verified the interaction 460
between the endogenous FL TDP-43 and the exogenous 461
Flag-tagged TDP-43. We excluded non-specific binding 462
of TDP-43 to immunoglobulins. We identified the 463
N-terminal half spanning amino acid residues 3–183 as 464
an intermolecular interacting domain. Finally, the 86-kDa 465
protein was identified in human brain tissues of various 466
neurological diseases, arguing against the possibility of 467
an in vitro artificial byproduct. Nevertheless, we 468
could not completely exclude the possibility that the 469
86-kDa protein represents a complex of TDP-43 with an 470
unidentified 43-kDa protein. It is of particular interest 471
that SDS-resistant dimers of DJ-1, whose loss of function 472
causes PD, are accumulated in PD and AD brains (Choi 473
et al. 2006). 474

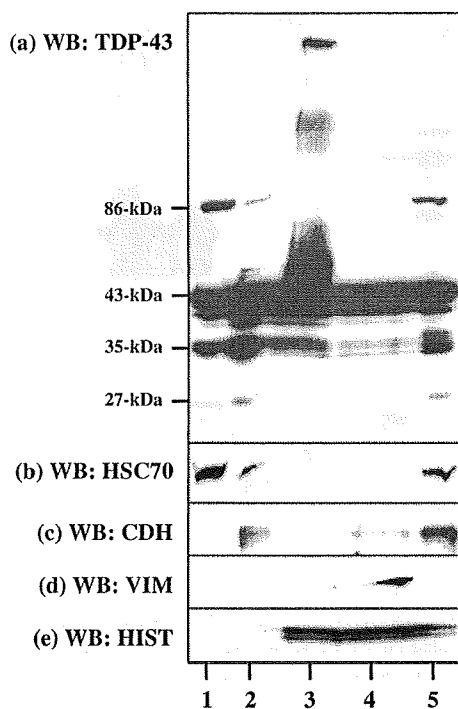


Fig. 5 Fractionation analysis of cellular proteins of HEK293. The cellular proteins of HEK293 separated into cytosol (lane 1), membrane (lane 2), nuclear (lane 3), and cytoskeletal (lane 4) fractions were processed for Western blot with anti-TDP-43 antibody (panel a), anti-HSC70 antibody (panel b), anti-pan-cadherin antibody (panel c), anti-vimentin antibody (panel d), and anti-histone H1 antibody (panel e). The lane (5) represents the unfraktionated input control

475 Supporting our observations, a recent crystal structural
 476 study has clarified the self-assembling capacity of TDP-43
 477 (Kuo et al. 2009). Another study showed that Flag-tagged
 478 FL TDP-43 protein binds to GFP-tagged C-terminally
 479 deleted products of TDP-43, suggesting a role of the

N-terminal domain in the intermolecular interaction
 (Zhang et al. 2009). In contrast, a different study disclosed
 that the wild-type human TDP-43 protein has an intrinsi-
 cally aggregation-prone propensity that requires the
 C-terminal domain (Johnson et al. 2009). Furthermore,
 DsRed-tagged FL TDP-43 is colocalized in cytoplasmic
 inclusions with GFP-tagged C-terminal fragments (Nonaka
 et al. 2009a). These observations suggest the possibility
 that the dimer formation of TDP-43 requires the N-terminal
 half, while afterward the aggregate formation involves the
 C-terminal domain as well.

In contrast to the normal nuclear location of TDP-43
 under physiological conditions, the pathogenic TDP-43 is
 often redistributed in the neuronal and glial cytoplasm and
 dystrophic neuritis by forming insoluble aggregates (Arai
 et al. 2006; Neumann et al. 2006). Importantly, we found
 that the 86-kDa TDP-43 dimer was enriched in the cyto-
 solic fraction in HEK293 cells. When the 86-kDa tan-
 demly connected dimer of TDP-43 was overexpressed in
 HEK293, it also showed a trend for being distributed out-
 side the nucleus, and promoted an accumulation of high-
 molecular-mass TDP-43-immunoreactive proteins. These
 observations propose the working hypothesis that a very
 small amount of TDP-43 dimer expressed constitutively in
 normal cells under physiological conditions might serve as
 a starting seed that triggers aggregation of posttransla-
 tionally modified TDP-43 species under pathological con-
 ditions of TDP-43 proteinopathy.

A previous study showed that TDP-43 continuously
 shuttles between the nucleus and the cytoplasm in a tran-
 scription-dependent manner (Ayala et al. 2008). Because
 TDP-43 plays a key role in shuttling of mRNA species in
 response to the neuronal injury (Moisse et al. 2009),
 even a trivial perturbation affecting the nucleocytoplasmic

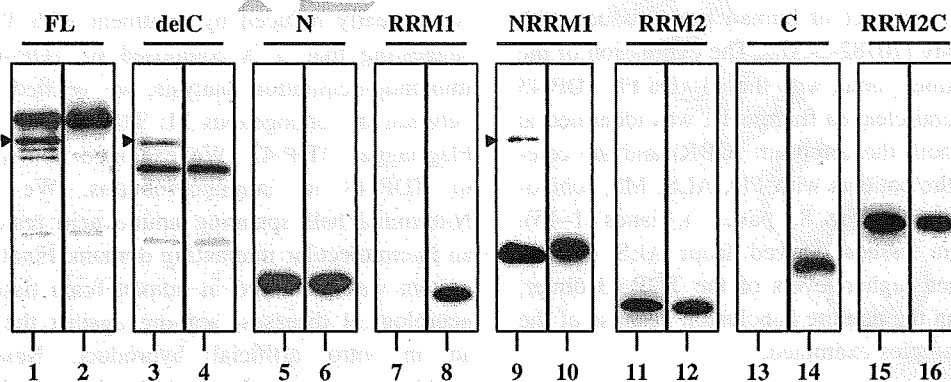


Fig. 6 The domains involved in the intermolecular interaction of TDP-43 proteins. Flag-tagged FL TDP-43 (lanes 1 and 2) and a panel of truncated proteins (see the details in Fig. 1), including delC (lanes 3 and 4), N (lanes 5 and 6), RRM1 (lanes 7 and 8), NRRM1 (lanes 9 and 10), RRM2 (lanes 11 and 12), C (lanes 13 and 14), and RRM2C (lanes 15 and 16) were individually expressed in HEK293 cells. The

protein extract was processed for IP with anti-Flag affinity gel, followed by Western blot with anti-TDP-43 antibody (lanes 1, 3, 5, 7, 9, 11, 13, and 15) or anti-Flag M2 antibody (lanes 2, 4, 6, 8, 10, 12, 14, and 16). The position (43-kDa) of the immunoprecipitated endogenous FL TDP-43 is indicated by arrow heads

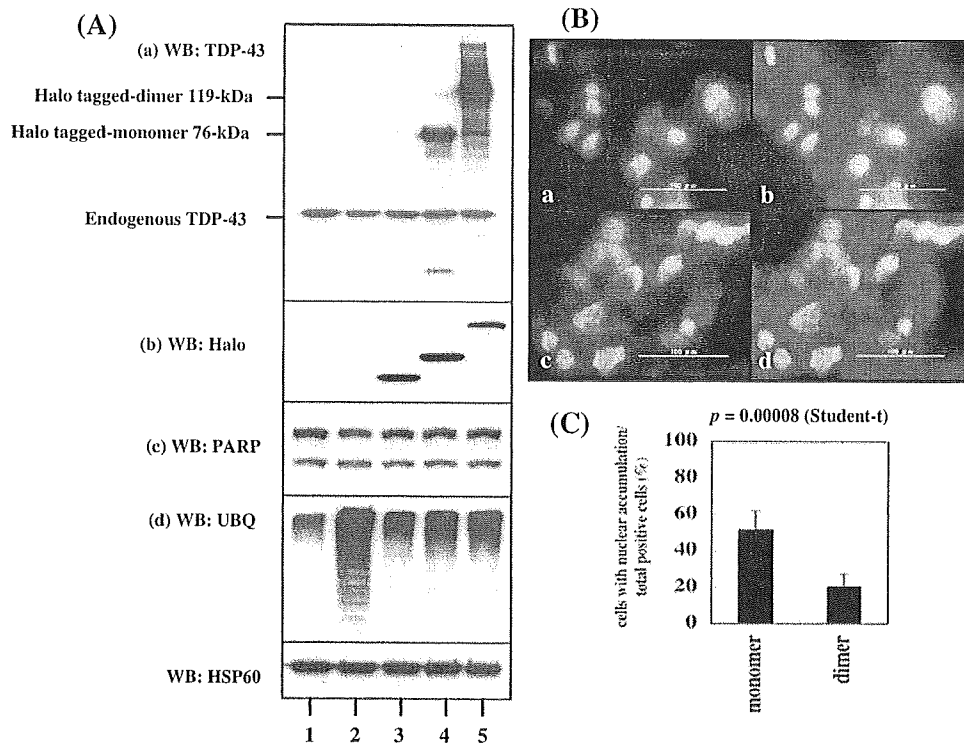
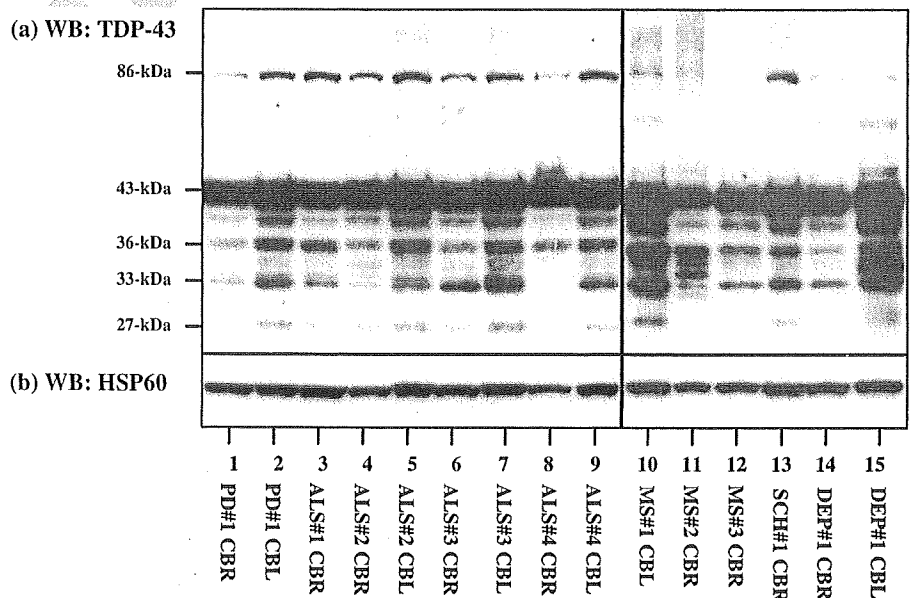


Fig. 7 TDP-43 dimer serves as a seed for promoting aggregation of TDP-43 proteins. **A** The expression of TDP-43 tandem dimer promotes an accumulation of high-molecular-mass TDP-43-immunoreactive proteins. The vectors of Halo-tagged GFP (lane 3), TDP-43 FL monomer (lane 4), or FL tandem dimer (lane 5) were transfected or untransfected (lanes 1 and 2) in HEK293 cells with (lane 2) or without (lanes 1, 3–5) a 24-h treatment of 1- μ M MG-132. The protein extract was processed for Western blot with anti-TDP43 antibody (panel a), anti-Halo tag antibody (panel b), anti-PARP antibody

(panel c), anti-ubiquitin antibody (panel d), or anti-HSP60 antibody, an internal control for protein loading (panel e). **B** Cell imaging analysis. HEK293 cells expressing Halo-tagged TDP-43 monomer (panels a and b) or tandem dimer (panels c and d) were processed for labeling with Oregon Green (panels a and c) merged with nuclear labeling with DAPI (panels b and d). **C** The counting of the number of the cells with nuclear accumulation of Halo-tagged proteins. The average of cell counts of six random fields under the magnification of $\times 400$ is shown with standard deviations

Fig. 8 The constitutive expression of TDP-43 dimer in human brain tissues. The detergent-soluble protein extract of human brain tissues of the cerebrum (CBR) (lanes 1, 3, 4, 6, 8, 11–14) and the cerebellum (CBL) (lanes 2, 5, 7, 9, 10, 15), derived from PD#1 (lanes 1 and 2), ALS#1 (lane 3), ALS#2 (lanes 4 and 5), ALS#3 (lanes 6 and 7), ALS#4 (lanes 8 and 9), MS#1 (lane 10), MS#2 (lane 11), MS#3 (lane 12), SCH#1 (lane 13), and DEP#1 (lanes 14 and 15) was processed for Western blot with anti-TDP43 antibody (upper panels) or anti-HSP60 antibody, an internal control for protein loading (lower panels)



514 transport of TDP-43 could disturb neuronal function by
 515 deregulating gene expression. TDP-43 accumulates in the
 516 cytoplasm following inhibition of RNA polymerase II by
 517 treatment with actinomycin D (Ayala et al. 2008). The
 518 C-terminal domain is the most important part for mainte-
 519 nance of solubility and cellular localization of TDP-43,
 520 while disruption of the RRM1 domain increases TDP-43
 521 binding to the chromatin and nuclear matrix (Ayala et al.
 522 2008). The TDP-43 mutant protein defective in the nuclear
 523 localization signal (NLS) forms cytoplasmic aggregates,
 524 while the mutant defective in the nuclear export signal
 525 (NES) constitutes nuclear aggregates (Winton et al. 2008).
 526 Inhibition of proteasome function by MG-132 enhances the
 527 aggregate formation in the NLS-defective mutant (Nonaka
 528 et al. 2009b). The overexpression of TDP-43 C-terminal
 529 fragment is sufficient to generate hyperphosphorylated and
 530 ubiquitinated cytoplasmic aggregates that could alter the
 531 exon splicing pattern (Zhang et al. 2009). Although over-
 532 expression of the wild-type human TDP-43 protein is toxic
 533 to yeast and rat cells (Johnson et al. 2008; Tatom et al.
 534 2009), overexpression of the tandem dimer of TDP-43 did
 535 not cause acute cytotoxicity in HEK293 cells in this study.

536 In this study, the levels of expression of TDP-43 dimer
 537 were unaltered in HEK293 cells by treatment with MG-132 or
 538 overexpression of ubiquilin-1 (UBQLN1). The ubiquilin family
 539 proteins, composed of an N-terminus ubiquitin-like (UBL)
 540 domain and a C-terminal ubiquitin-associated (UBA) domain
 541 separated by a central Sti I-like repeat, physically interact with
 542 both proteasomes and ubiquitin ligases (Ford and Monteiro
 543 2006). UBQLN1, capable of forming a dimer via the central
 544 region, promotes the formation of cytoplasmic aggregates of
 545 TDP-43, and regulates the proteasome and autophagosome
 546 targeting of TDP-43 aggregates (Kim et al. 2008). Polyubiq-
 547 uitinated TDP-43 interacts with the UBA domain of UBQLN1
 548 (Kim et al. 2008). We found that following the expression of
 549 the tandem TDP-43 dimer, accumulated high-molecular-mass
 550 TDP-43-immunoreactive proteins are unlikely to be ubiqui-
 551 tinated. The 86-kDa TDP-43 dimer constitutively expressed in
 552 cultured human cells might not interact with UBQLN1,
 553 because it is unlikely to be modified by polyubiquitination.

554 The present observations suggest that the 86-kDa TDP-
 555 43-immunoreactive protein represents a very small amount
 556 of dimerized TDP-43 expressed constitutively in normal
 557 cells under physiological conditions. We suppose that this
 558 dimerized TDP-43 might serve as a starting seed that
 559 triggers aggregation of TDP-43 under pathological condi-
 560 tions of TDP-43 proteinopathy. This hypothesis warrants
 561 further immunohistochemical and neurochemical investi-
 562 gations, including the establishment of TDP-43-dimer-
 563 specific antibodies.

564 **Acknowledgments** Human brain tissues were provided by Research
 565 Resource Network (RRN), Japan. This work was supported by a

research grant to J-IS from the High-Tech Research Center Project,
 the Ministry of Education, Culture, Sports, Science and Technology
 (MEXT), Japan (S0801043) and a grant from Research on Intractable
 Diseases, the Ministry of Health, Labour and Welfare of Japan.

References

- Arai T, Hasegawa M, Akiyama H, Ikeda K, Nonaka T, Mori H, Mann D, Tsuchiya K, Yoshida M, Hashizume Y, Oda T (2006) TDP-43 is a component of ubiquitin-positive tau-negative inclusions in frontotemporal lobar degeneration and amyotrophic lateral sclerosis. *Biochem Biophys Res Commun* 351:602–611
- Ayala YM, Pantano S, D'Ambrogio A, Buratti E, Brindisi A, Marchetti C, Romano M, Baralle FE (2005) Human, *Drosophila*, and *C. elegans* TDP43: nucleic acid binding properties and splicing regulatory function. *J Mol Biol* 348:575–588
- Ayala YM, Zago P, D'Ambrogio A, Xu YF, Petrucelli L, Buratti E, Baralle FE (2008) Structural determinants of the cellular localization and shuttling of TDP-43. *J Cell Sci* 121:3778–3785
- Buratti E, Baralle FE (2008) Multiple roles of TDP-43 in gene expression, splicing regulation, and human disease. *Front Biosci* 13:867–878
- Buratti E, Brindisi A, Giombi M, Tisminetzky S, Ayala YM, Baralle FE (2005) TDP-43 binds heterogeneous nuclear ribonucleoprotein A/B through its C-terminal tail: an important region for the inhibition of cystic fibrosis transmembrane conductance regulator exon 9 splicing. *J Biol Chem* 280:37572–37584
- Choi J, Sullards MC, Olzmann JA, Rees HD, Weintraub ST, Bostwick DE, Gearing M, Levey AI, Chin LS, Li L (2006) Oxidative damage of DJ-1 is linked to sporadic Parkinson and Alzheimer diseases. *J Biol Chem* 281:10816–10824
- Ford DL, Monteiro MJ (2006) Dimerization of ubiquilin is dependent upon the central region of the protein: evidence that the monomer, but not the dimer, is involved in binding presenilins. *Biochem J* 399:397–404
- Geser F, Martinez-Lage M, Kwong LK, Lee VM, Trojanowski JQ (2009) Amyotrophic lateral sclerosis, frontotemporal dementia and beyond: the TDP-43 diseases. *J Neurol* 256:1205–1214
- Hasegawa M, Arai T, Nonaka T, Kametani F, Yoshida M, Hashizume Y, Beach TG, Buratti E, Baralle F, Morita M, Nakano I, Oda T, Tsuchiya K, Akiyama H (2008) Phosphorylated TDP-43 in frontotemporal lobar degeneration and amyotrophic lateral sclerosis. *Ann Neurol* 64:60–70
- Johnson BS, McCaffery JM, Lindquist S, Gitler AD (2008) A yeast TDP-43 proteinopathy model: exploring the molecular determinants of TDP-43 aggregation and cellular toxicity. *Proc Natl Acad Sci USA* 105:6439–6444
- Johnson BS, Snead D, Lee JJ, McCaffery JM, Shorter J, Gitler AD (2009) TDP-43 is intrinsically aggregation-prone and ALS-linked mutations accelerate aggregation and increase toxicity. *J Biol Chem* 284:20329–20339
- Kabashi E, Valdmanis PN, Dion P, Spiegelman D, McConkey BJ, Vande Velde C, Bouchard JP, Lacomblez L, Pochigaeva K, Salachas F, Pradat PF, Camu W, Meininger V, Dupre N, Rouleau GA (2008) TARDBP mutations in individuals with sporadic and familial amyotrophic lateral sclerosis. *Nat Genet* 40:572–574
- Kametani F, Nonaka T, Suzuki T, Arai T, Dohmae N, Akiyama H, Hasegawa M (2009) Identification of casein kinase-1 phosphorylation sites on TDP-43. *Biochem Biophys Res Commun* 382:405–409
- Kim SH, Shi Y, Hanson KA, Williams LM, Sakasai R, Bowler MJ, Tibbetts RS (2008) Potentiation of ALS-associated TDP-43

- 628 aggregation by the proteasome-targeting factor, Ubiquilin 1. *J Biol Chem* 284:8083–8092
- 629
- 630 Kuo PH, Doudeva LG, Wang YT, Shen CK, Yuan HS (2009)
- 631 Structural insights into TDP-43 in nucleic-acid binding and
- 632 domain interactions. *Nucleic Acids Res* 37:1799–1808
- 633 Moisse K, Volkening K, Leystra-Lantz C, Welch I, Hill T, Strong MJ
- 634 (2009) Divergent patterns of cytosolic TDP-43 and neuronal
- 635 progranulin expression following axotomy: implications for
- 636 TDP-43 in the physiological response to neuronal injury. *Brain*
- 637 *Res* 1249:202–211
- 638 Neumann M, Sampathu DM, Kwong LK, Truax AC, Micsenyi MC,
- 639 Chou TT, Bruce J, Schuck T, Grossman M, Clark CM,
- 640 McCluskey LF, Miller BL, Masliah E, Mackenzie IR, Feldman
- 641 H, Feiden W, Kretzschmar HA, Trojanowski JQ, Lee VM (2006)
- 642 Ubiquitinated TDP-43 in frontotemporal lobar degeneration and
- 643 amyotrophic lateral sclerosis. *Science* 314:130–133
- 644 Neumann M, Kwong LK, Lee EB, Kremmer E, Flatley A, Xu Y,
- 645 Forman MS, Troost D, Kretzschmar HA, Trojanowski JQ, Lee
- 646 VM (2009) Phosphorylation of S409/410 of TDP-43 is a
- 647 consistent feature in all sporadic and familial forms of TDP-43
- 648 proteinopathies. *Acta Neuropathol* 117:137–149
- 649 Nonaka T, Kametani F, Arai T, Akiyama H, Hasegawa M (2009a)
- 650 Truncation and pathogenic mutations facilitate the formation of
- 651 intracellular aggregates of TDP-43. *Hum Mol Genet* 18:3353–
- 652 3364
- 653 Nonaka T, Arai T, Buratti E, Baralle FE, Akiyama H, Hasegawa M
- 654 (2009b) Phosphorylated and ubiquitinated TDP-43 pathological
- 655 inclusions in ALS and FTL-DU are recapitulated in SH-SY5Y
- 656 cells. *FEBS Lett* 583:394–400
- Ou SH, Wu F, Harrich D, García-Martínez LF, Gaynor RB (1995) 657
Cloning and characterization of a novel cellular protein, TDP-43, 658
that binds to human immunodeficiency virus type 1 TAR DNA 659
sequence motifs. *J Virol* 69:3584–3596 660
- Satoh J, Obayashi S, Misawa T, Sumiyoshi K, Oosumi K, Tabunoki H 661
(2009) Protein microarray analysis identifies human cellular 662
prion protein interactors. *Neuropathol Appl Neurobiol* 35:16–35 663
- Tatom JB, Wang DB, Dayton RD, Skalli O, Hutton ML, Dickson 664
DW, Klein RL (2009) Mimicking aspects of frontotemporal 665
lobar degeneration and Lou Gehrig's disease in rats via TDP-43 666
overexpression. *Mol Ther* 17:607–613 667
- Wang IF, Wu LS, Shen CK (2008) TDP-43: an emerging new player 668
in neurodegenerative diseases. *Trends Mol Med* 14:479–485 669
- Winton MJ, Igaz LM, Wong MM, Kwong LK, Trojanowski JQ, Lee 670
VM (2008) Disturbance of nuclear and cytoplasmic TAR DNA- 671
binding protein (TDP-43) induces disease-like redistribution, 672
sequestration, and aggregate formation. *J Biol Chem* 283:13302– 673
13309 674
- Zhang YJ, Xu YF, Dickey CA, Buratti E, Baralle F, Bailey R, 675
Pickering-Brown S, Dickson D, Petrucelli L (2007) Progranulin 676
mediates caspase-dependent cleavage of TAR DNA binding 677
protein-43. *J Neurosci* 27:10530–10534 678
- Zhang YJ, Xu YF, Cook C, Gendron TF, Roettges P, Link CD, Lin 679
WL, Tong J, Castaneda-Casey M, Ash P, Gass J, Rangachari V, 680
Buratti E, Baralle F, Golde TE, Dickson DW, Petrucelli L (2009) 681
Aberrant cleavage of TDP-43 enhances aggregation and cellular 682
toxicity. *Proc Natl Acad Sci USA* 106:7607–7612 683
684

Neuropathology and Applied Neurobiology

NAN-2009-0116 Revised

Original Article**Full Title:****Aberrant microRNA expression in the brains of neurodegenerative diseases:
miR-29a decreased in Alzheimer disease brains targets neuron navigator-3****M. Shioya^{*}, S. Obayashi^{*}, H. Tabunoki^{*}, K. Arima[†], Y. Saitoh[‡], T. Ishida[§] and J.
Satoh^{*}**

^{}Department of Bioinformatics and Molecular Neuropathology, Meiji Pharmaceutical University, Tokyo, Japan, [†]Department of Psychiatry, National Center Hospital, NCNP, Tokyo, Japan, [‡]Department of Laboratory Medicine, National Center Hospital, NCNP, Tokyo, Japan, [§]Department of Pathology and Laboratory Medicine, Kohnodai Hospital, International Medical Center, Chiba, Japan*

Correspondence: Jun-ichi Satoh, Department of Bioinformatics and Molecular Neuropathology, Meiji Pharmaceutical University, 2-522-1 Noshio, Kiyose, Tokyo 204-8588, Japan.

Tel: +81 42 4958678; fax: +81 42 4958678; E-mail: satoj@my-pharm.ac.jp.

Running Title: Aberrant miRNA expression in neurodegenerative disease brains

The manuscript is composed of the text (22 pages), five figures, two tables, and three supplementary tables for online presentation only.